Journal of Materials Chemistry C

Accepted Manuscript

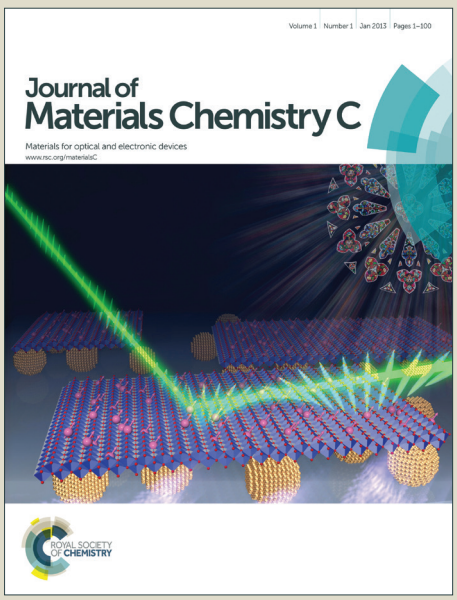

ROYAL SOCIETY OF CHEMISTRY

www.rsc.org/materialsC

Journal of
Materials Chemistry C

RSCPublishing

Ordering Dynamics in Symmetric PS-b-PMMA Diblock Copolymer Thin Films During Rapid Thermal Processing

,Cite this: DOI: 10.1039/x0xx00000x

Received ooth January 2012,
Accepted ooth January 2012

DOI: 10.1039/x0xx00000x

www.rsc.org/

Michele Perego [a*], Federico Ferrarese Lupi [a], Monica Ceresoli [a,b], Tommaso Jacopo Giammaria[a], Gabriele Seguini[a], Emanuele Enrico [c], Luca Boarino[c], Diego Antonioli[d], Valentina Gianotti[d], Katia Sparnacci[d], Michele Laus[d*]

The pattern coarsening dynamics in symmetric polystyrene-b-polymethylmethacrylate (PS-b-PMMA) block copolymer thin films under conventional thermal treatments is extremely slow, resulting in limited correlation length values even after prolonged annealing at relatively high temperatures. This study describes the kinetics of symmetric block copolymer microphase separation when subjected to a thermal treatment based on the use of a Rapid Thermal Processing (RTP) system. The proposed methodology allows self-organizing symmetric PS-b-PMMA thin films in few seconds, taking advantage of the amount of solvent naturally trapped within the film during the spinning process. Distinct and self-registered morphologies, coexisting along the sample thickness, are obtained in symmetric PS-b-PMMA samples, with periodic lamellae laying over a hexagonal pattern of PMMA cylinders embedded in the PS matrix and perpendicularly oriented with respect to the substrate. The ordering dynamics and morphological evolution of the coexisting dual structures are delineated and the intimate mechanism of the self-assembly and coarsening processes are discussed and elucidated.

Introduction

Block copolymers are appealing self-organizing materials for nanotechnology applications, since they spontaneously phase separate into a rich variety of periodic structures with typical feature size below 50 nm.[1,2] In the form of thin films, they have attracted considerable interest as they are compatible with conventional fabrication protocols of semiconductor industries[3-7] and, consequently, they could represent the operative tool for the development of dense, high aspect ratio patterns in the next generation of microelectronic and data storage devices. In this regard, a special place is held by thin films of symmetric block copolymers leading to lamellar structures because of their advantageous profile for lithographic applications involving striped patterns. However, till now, the slow evolution with time of symmetric block copolymers under conventional thermal treatments significantly limited their implementation in applications requiring long-range order.[8,9] To address the problem, alternative approaches have been proposed to drive the self-assembly like, for instance, the so called solvent annealing. This approach demonstrated the capability to control the ordering and orientation of microdomains in thin films of block copolymers but its possible implementation in industrial like environments is everything but trivial. On the other hand topographical or chemical constrains were introduced in the substrate to drive the ordering during conventional thermal treatments.[10–18] This surface pre-patterning demonstrated to be effective in directing the self-assembly process and achieving long range ordering in relatively short time periods.[19] Nevertheless, for some applications, the organization of block copolymers on featureless regions of the surface is required and a general route toward rapid ordering is fundamental.[20-22]

The ordering mechanism of the block copolymer microdomains on unpatterned substrates has been the subject of an intense research activity.[8,9,16,23–31] Coarsening in block copolymers occurs via defect motion and annihilation that finally implies the diffusion of macromolecules. In microphase separated systems, molecular diffusion occurring along the microdomains is favored over diffusion across the microdomains because of the enthalpy barrier to block copolymer mixing. Literature data indicate that fast coarsening occurs in asymmetric block copolymers leading to parallel or perpendicular cylinder morphologies.[20–22,23,25] In contrast, short correlation lengths are reported for the perpendicular lamellae morphology of symmetric block copolymers.[8–11] The very limited time and temperature dependence of the correlation length strongly reduces the capability of improving long range ordering and of reducing the defectiveness of the morphological arrangement.[3] The fast coarsening kinetics in cylindrical morphologies is strictly related to their particular topology, since the matrix of the cylindrical phase provides a simple channel for layer breaking by molecular motion around the cylinder cores. On the contrary, in lamellar morphologies, defect annihilation requires layer breaking with molecular diffusion across the microdomains resulting in a high activation energy for the annihilation process and in a slow rate of pattern coarsening and ordering development.[8,24]

In this work, the pattern coarsening dynamics in thin films of a symmetric polystyrene-b-polymethylmethacrylate (PS-b-

PMMA) block copolymer is investigated as a function of annealing temperature (T_a) and time (t_a). The infrared radiation of a Rapid Thermal Processing (RTP) apparatus is employed to govern the temperature of the polymeric films.[29] Using this technology, the sample temperature can be driven well above the glass transition (T_g), stabilized at the desired ordering temperature and finally decreased below T_g in few seconds, thus preventing any significant degradation of the polymeric material. The grain coarsening of the perpendicular lamellae is measured as a function of the annealing temperature and time. The dynamics of pattern coarsening is correlated to the peculiar morphology evolution of the polymeric film and to the residual solvent, which is naturally trapped in the polymeric film during the spin coating procedure.

Experimental

Materials. The hydroxyl terminated poly(styrene-r-methylmethacrylate) (P(S-r-MMA)) random copolymer with styrene fraction $X_S = 0.58$ (M_n = 11400 g/mol, PDI = 1.64) and the block copolymer PS-b-PMMA with styrene fraction of X_S = 0.5 (symmetric copolymer, M_n = 51000 g/mol and PDI = 1.06, PMMA syndiotactic rich contents > 78%) were purchased from Polymer Source Inc. and used as obtained. These copolymers were marked as R58 and B50 were R and B stand for random and block, respectively, and the number represents the percent styrene unit.

Sample Preparation. The substrates consist of square pieces of about 1 cm^2 of oriented silicon (100) featuring a 100 nm thick thermal SiO_2 layer. Prior to random copolymer deposition, each substrate was cleaned with Piranha solution (H_2SO_4/H_2O_2 with 3/1 vol. ratio at 80°C for 40 min), rinsed in H_2O and finally dried under N_2 flow. The cleaning process was completed by an ultrasonic bath in 2-propanol. After the cleaning process, a solution of R58 (18.0 mg in 2.0 mL of toluene) was prepared, sonicated in an ultrasonic bath, and then spun on the substrates for 30 s at 3000 rpm. In these conditions, a random copolymer film with thickness around 30 nm is obtained. The grafting reaction was performed by RTP treatment (Jipelec, JetFirst Series rapid thermal processing system) of 600 s at 250°C under N_2 atmosphere. In a recent paper, we reported a detailed study about the kinetics of the grafting process at high temperature in a RTP apparatus.[30] The removal of the non-grafted R58 was performed by ultrasonic bath in toluene. Finally the samples were dried under N_2 flow. On the grafted R58, a solution of B50 (18.0 mg in 2.0 mL of toluene) was spun for 30 s at 3000 rpm resulting in a polymeric film of ~ 26 nm. The samples were subjected to different RTP treatments, setting the final annealing temperature between 250 and 290°C, with annealing time ranging from 1 s to 1200 s. In all treatments, the heating ramp was fixed at 18°C/s.

Morphological Characterization. The thickness of all the polymeric films was measured before and after the RTP treatment by a M-200U spectroscopic ellipsometer (J. A. Wollam Co. Inc.) using a Xenon lamp at 70° incident angle. The morphological characterization of the self-assembled block copolymer films was performed by Scanning Electron Microscopy (SEM) (Zeiss Supra 40 system). In order to increase the contrast in the SEM analysis and to carry out a depth profiling of the film morphology, a selective etching of the PMMA block was performed by exposing the samples to UV radiation (5 mW/cm^2, λ = 253.7 nm) for different time periods and subsequently rinsing them in an acetic acid solution. The quantitative determination of the level of organization in lamellar thin films was obtained measuring the correlation length of the striped pattern according to the methodology originally proposed by Harrison et al.[23,24] The appropriate magnification was selected so that the SEM image size is at least 15 times larger than the correlation length and the image resolution was properly set in order to maintain a good nm/pixel ratio. To provide a statistical evaluation of the ordering in the block copolymer thin film, several SEM images in different areas of the sample were acquired and analyzed. STEM cross sectional image of the PS-b-PMMA block copolymer thin film after annealing in RTP at 250°C for 60 s. was performed on a sample that was prepared by standard FIB lift-out technique using a FEI Dualbeam Quanta 3D™.

Toluene Determination. The residual toluene in the as received bulk materials and in the films was determined by Gas Chromatography–Mass Spectrometry (GC-MS) after solvent extraction using dichloromethane. All the GC-MS analyses were performed using a Finnigan Trace GC Ultra coupled with a Trace DSQ Analyser. The GC separation was carried out using a Phenomenex DB5-5ms capillary column (30 m, 0.25 i.d., 0.25 thickness). The oven heating rate was 10°C/min from 45 to 110°C and 60°C/min from 110 to 180°C. The injector was set in split mode with a split ratio of 1:10 at the temperature of 250°C and under a constant flow (1.0 mL/min) of helium as the carrier gas. The transfer line temperature was set at 280°C. The MS signal was acquired in EI+ mode with an Ionization Energy of 70.0 eV and the ion source temperature at 250°C. The acquisition was performed both in full-scan mode, in the 20-450 m/z range, and in Single Ion Monitoring (SIM) mode (92 m/z). The SIM signal was used in the quantification process by integration of the chromatographic peak, identified by comparison with the retention time and mass spectrum of a standard toluene solution. The quantification was carried out both by performing a toluene calibration curve in the suitable concentration range and by the response factor method using anisole as the Internal Standard (IS). The IS was added to all the samples at the concentration of 0.2 mg/L and was monitored in SIM acquisition at 108 m/z.
In case of R58 and B50 bulk materials, 1.0 mg of each copolymer was dissolved in 1.0 mL of dichloromethane for 48 hours. Then, the solution was filtered and 3.0 μL were injected in the gas chromatograph. The as-received R58 and B50 samples contain small amounts of toluene, which resulted 120.0 and 43.1 μg/Kg, respectively. In the case of thin films, each sample stood in contact with 1.0 mL of dichloromethane for 24 hours. Then, the dichloromethane was replaced with another aliquot of 1.0 mL of fresh dichloromethane and, after additional 24 hours extraction time, the two aliquots were combined, the final solution filtered and 3.0 μL injected into the GC-MS.
The toluene amount was reported as relative volume amount of solvent retained (% V_r) calculated as follow:

$$\%V_r = [V_t/V_{total}] * 100$$

where V_{total} is the total volume of the polymeric material and toluene estimated from the thickness of the film and the area of the substrate and V_t stands for the toluene volume retained in the film, calculated from the absolute amount of toluene M_t,

$$V_t = M_t/\rho_t$$

where ρ_t is the bulk density of toluene (0.867 g/ml).

Result and discussion

Pattern evolution. Figure 1 reports the sequence of SEM images illustrating the time evolution of the lamellae microdomains at T_a = 250, 270, and 290°C. Measurements at temperatures higher than 290°C were prevented by the degradation of the random copolymer brush layer.[31] For the shortest annealing time (t_a = 1 s), a clear signature of phase separation is observed at all annealing temperatures, although the specific temperature affects both the lateral ordering and the morphology within the microdomains. In fact, poor lamellae ordering is observed in the sample annealed at 250°C whereas, in the samples annealed at 270 and 290°C, the lamellae are much more defined. In addition, in the samples annealed at 250 and 270°C, a peculiar morphology is observed including both cylinders and lamellae perpendicularly oriented to the substrate. Conversely, in the sample annealed at 290°C, small size lamellae microdomains are mainly detected and only few and isolated cylinders are distinguishable.

It is important to recognize that all the samples were heated up at the constant heating rate of 18°C/s, which corresponds to about 5 s heating time to move the system from a temperature at which the ordering is extremely slow (about 170°C) to the final target temperature. Consequently, the 1 s annealing time is almost negligible compared to the overall thermal budget and the corresponding morphologies should be considered just as snapshots of the evolution of the system during the heating and cooling stages. In this frame, although a complete picture of the system evolution during the transient stages is still lacking, the above data suggest a well-defined path for striped pattern formation involving a transition through a perforated lamellar phase that rapidly evolves to the final lamellar morphology, in agreement with previously reported data on symmetric PS-b-PMMA at 190°C.[29] For $t_a \geq 5$ s, no more evidence of perforated lamellae is observed and the samples show well-defined lamellar microdomains, perpendicularly oriented with respect to the substrate.

The lateral organization of the lamellar domains depends on the annealing temperature and time. Within this time frame, the high temperature isothermal stage predominates over the initial transient period and drives the system evolution towards the final thermodynamic equilibrium condition. In particular, irrespective of the annealing temperature, a progressive and significant reduction of defect density is observed as the annealing time increases, thus ultimately leading to an increase in the ordering level within the striped patterns.

According to the SEM images reported in Figure 1, the self-assembly process in the block copolymer thin film exhibits a strong time and temperature dependence, in contrast with previously reported data.[8–10] To monitor the coarsening of the lamellae microdomains at different annealing temperatures as a function of time, the correlation length ξ values were determined from the above SEM images, following the procedure described in literature,[24,32] and are collectively reported in Figure 2 for the different annealing temperatures T_a. The correlation length ξ values of the samples annealed at 250°C for 1 and 5 s and of the sample annealed at 270°C for 1 s are not included, since their low ordering degree prevented the accurate determination of the correct ξ values. Moreover, in case of the samples annealed at 290°C, the point corresponding

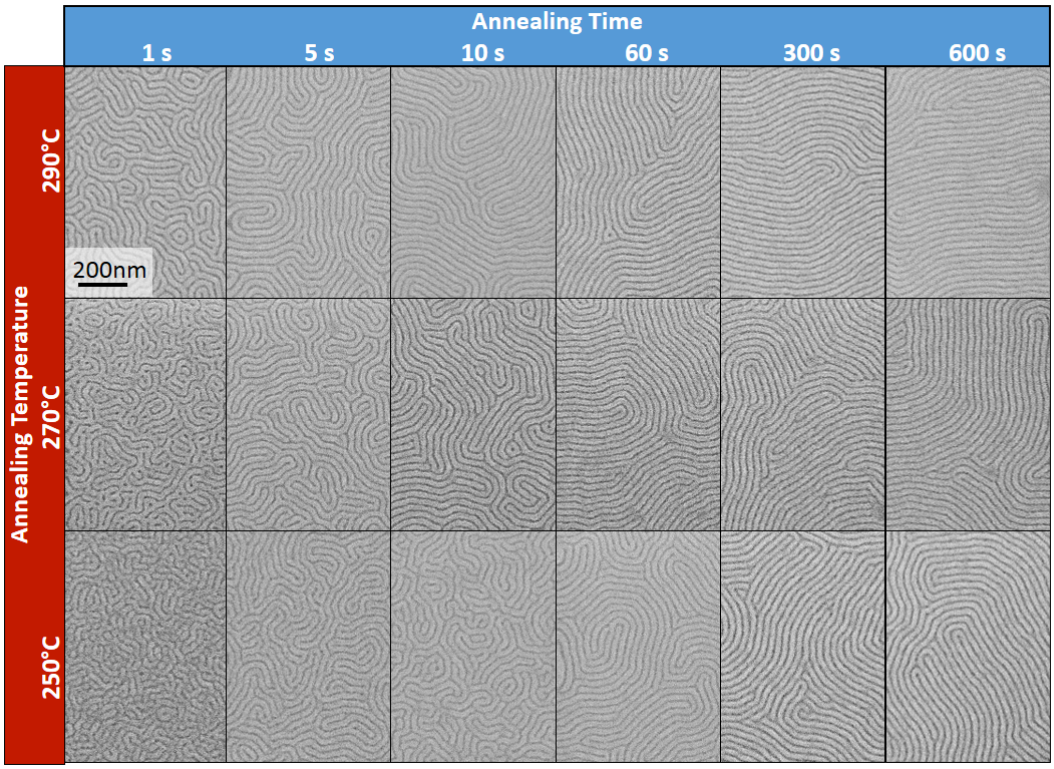

Fig. 1 Plan view SEM images of B50 films annealed at different temperatures (T_a = 250, 270, and 290°C) for different time periods (t_a from 1 to 600 s). The images were acquired after oxygen plasma-etching steps of 60 s in order to remove the PMMA phase and enhance the contrast.

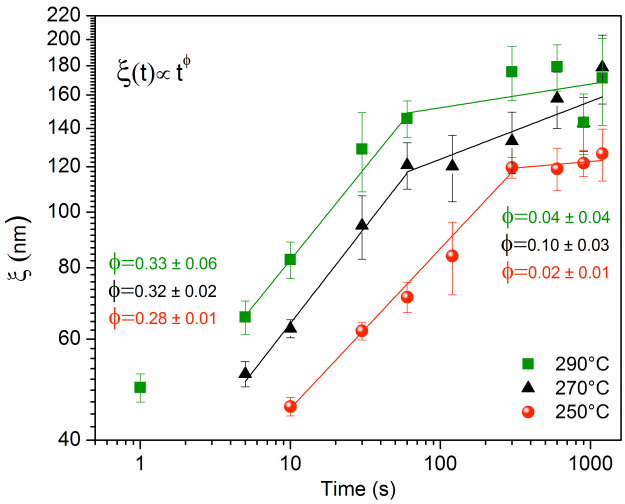

Fig. 2 Correlation length ξ of lamellar pattern of B50 thin films as a function of the annealing time at different temperatures.

to t_a = 1 s has not been included in the power law fitting of the data, since it is not representative of the evolution of the system in the isothermal stage but typifies the result of the system evolution during the transient stage.

Irrespective of the temperature, the correlation length increases steeply at first and then more gradually as a function of t_a, with a well-defined threshold, which depends on the temperature, thus suggesting the occurrence of two distinct growth regimes. These two regimes are characterized by power laws with markedly different growth exponents (ϕ). In the fast coarsening regime, an average ϕ value of 0.29 ± 0.01 is determined whereas, in the slow coarsening regime, ϕ values are more scattered ranging from 0.02 ± 0.01 to 0.10 ± 0.03, with an average ϕ value 0.03 ± 0.01. The latter growth exponents are perfectly consistent with those reported in literature pointing to very limited or even no coarsening in perpendicularly oriented symmetric block copolymers.[8,9] In contrast, the growth exponent corresponding to the initial fast coarsening regime indicates a very effective coarsening process with experimental growth rates equivalent to those observed in sphere or cylinder forming block copolymers.[23,25] In the present system, the growth rate values measured during the fast ordering regime correspond to the maximum allowable value for non-entangled polymers having an interconnected matrix, as is the case of asymmetric block copolymer systems. In a somewhat parallel fashion, the growth exponents observed in the slow ordering regime equal those expected in the case of pattern formation in systems without an embedding matrix, as is the case of symmetric block copolymer systems. It is worth to note that the absolute values of the correlation lengths at relatively short annealing times (t_a = 60 s) are much higher than those reported in the literature, for the same block copolymer sample, after very long furnace annealing at the same temperatures. In particular, ξ values from 42 to 64 nm were reported by Ruiz et al. for annealing temperatures ranging from 180°C to 285°C and t_a = 6000 s, demonstrating a very limited temperature dependence of the final correlation length values.[11] In our experiment, ξ values well above 120 nm were obtained at all temperatures in a time scale that is two order of magnitude lower than the one reported by Ruiz and coworkers.[8]

Morphology Evolution. The morphology throughout the polymeric film was investigated by top-down SEM analysis after oxygen plasma-etching for different time periods. Figure 3 reports the plan view SEM images of the samples annealed at 250, 270, and 290°C for t_a = 1 and 600 s. The morphology of the samples is compared after oxygen plasma-etching times of 60 and 120 s. The SEM images reveal that, irrespective of the annealing temperature, in the samples annealed for 1 s (Figure 3, left row), the perpendicularly oriented lamellae did not propagate through the entire polymeric film and the samples exhibit two closely connected morphologies suggesting the presence of hexagonally packed PMMA cylinders perpendicularly oriented with respect to the substrate underlying the lamellar arrangement. In contrast, the samples annealed for 600 s (Figure 3, right side) exhibit no evidence of cylindrical phase even after prolonged plasma etching. In these samples, the removal of the PMMA phase produces a collapse of the structure due to the reduced mechanical stability of the PS lamellae after the removal of the PMMA phase, thus further supporting the idea that the lamellae spread through the entire film thickness.[33]

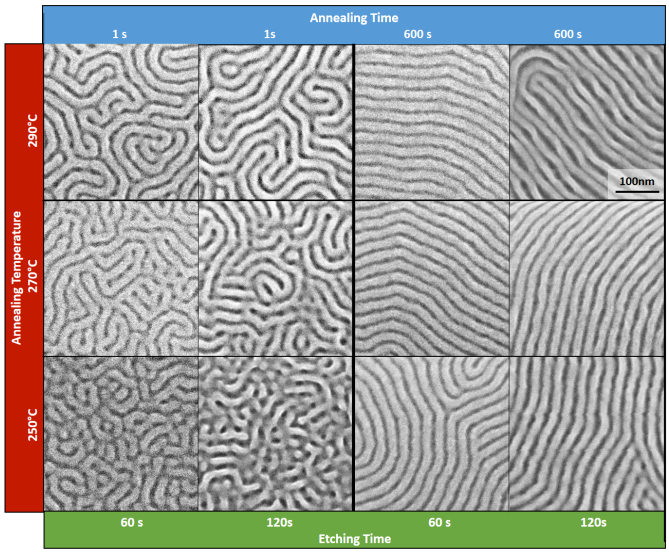

Fig. 3 SEM images of the samples annealed at 250, 270, and 290°C for 1 s (left) and 600 s (right) after oxygen plasma-etching steps of 60 s and 120 s respectively. For short annealing times, the lamellae did not propagate through the entire film thickness and the samples exhibit signature of a double-layer structure with lamellae at the top and cylinders at the bottom.

To better clarify the observed peculiar morphology, Figure 4(a) reports a SEM plan view image of the sample annealed at 250°C for 60 s, after prolonged oxygen plasma exposure. The removal of the PMMA phase clearly confirms the presence of a double morphology.

The Fast Fourier Trasform (FFT) of a small portion of the image (inset of Figure 4(a) indicates the existence of a phase with hexagonally packed PMMA cylinders that appears to be self-registered with the lamellar structures at the top of the surface. Further confirmation of this structure is provided by the cross-sectional STEM analysis of the same sample reported in figure 4(b). After the removal of the PMMA phase, the sample was prepared for STEM analysis and the polymeric layer was covered by a protective AuPd thin film. The bright underlying region in the picture corresponds to the substrate. The grey area on top shows the protective AuPd layer deposited that replaced the PMMA phase. The white dashed line indicates

the original thickness of the polymeric film. The cross sectional image confirms the presence of two closely connected lamellar and cylinder structures through the film thickness. The periodicity of the underlying cylindrical structures was determined to be around 27 nm, in good agreement with the characteristic length $L_0 \sim 27$ nm of the lamellar phase for this specific PS-b-PMMA block copolymer. This experimental evidence further supports the idea of a continuous evolution of the microdomain morphology along the direction perpendicular to the film thickness. The combination of plan and cross sectional images rules out the possibility of parallel cylinder formation at the surface of the polymeric film and clearly indicate that the morphology of the film is characterized by two closely connected lamellar and cylinder structures, as schematically represented in Figure 4(c). Surprisingly this picture is consistent with the one previously reported by Sakurai et al.[34] in the case of a thermally induced morphology transition from cylindrical to lamellar microdomains in bulk poly(styrene-b-butadiene-b-styrene) block copolymer samples. Despite the fact that di-block and tri-block copolymers have vastly different phase spaces, the similarities between the morphologies of the two systems suggest that a homologous mechanism could be accounted for the transition via coalescence of cylinders without translation of their center-of-mass.

Figure 5 describes the morphology evolution as a function of the annealing time in the samples annealed at 290°C, for three etching times (60, 120, and 210 s). After the short plasma-etching process (60 s), the presence of the cylindrical phase is evident only in the sample annealed for 1 s whereas, for longer annealing times, the SEM images reveal lamellae perpendicularly oriented to the substrate. After 120 s plasma-etching time, the SEM images returns a quite different picture indicating the presence of a cylinder phase also in samples annealed for 10 s. A further increase in the plasma-etching time (210 s) reveals a trace of a cylindrical phase even in the sample annealed for 60 s and finally demonstrates the absence of this phase in the polymeric films when the annealing time is longer than 60 s. The above data confirm the idea of two closely connected lamellar and cylinder structures and demonstrate that a transition from the cylindrical phase to the lamellar one occurs during the annealing process and matches the progressive increase in the lateral ordering of the film. Similar results were obtained for the films annealed at 270 and 250°C, with the disappearance of the cylindrical phase occurring at progressively higher t_a values when decreasing the annealing temperature.

Solvent dynamics. The occurrence of a cylinder morphology, in which the cylinders consist of PMMA, in a film of symmetric PS-b-PMMA block copolymer suggests that a consistent amount of toluene, which is a preferential solvent for the PS could be entrapped in the film.[35] A related, although reverse, situation was described in case of a symmetric PS-b-PMMA block copolymer solvent-annealed with the PMMA-selective acetone vapor.[36] In that case, the block copolymer films showed a parallel orientation of the cylindrical PS microdomains over the underlying perpendicular PS cylinders on the substrate. Successive thermal annealing allowed a structural reorganization to take place leading to the equilibrium morphology with the perpendicular orientation of the lamellar microdomains. It is worth to note that, in a recent paper, we observed the occurrence of orientation flipping of the nanodomains in cylinder forming PS-b-PMMA thin films confined within topographically defined structures during high temperature thermal treatments in a RTP machine.[37] This

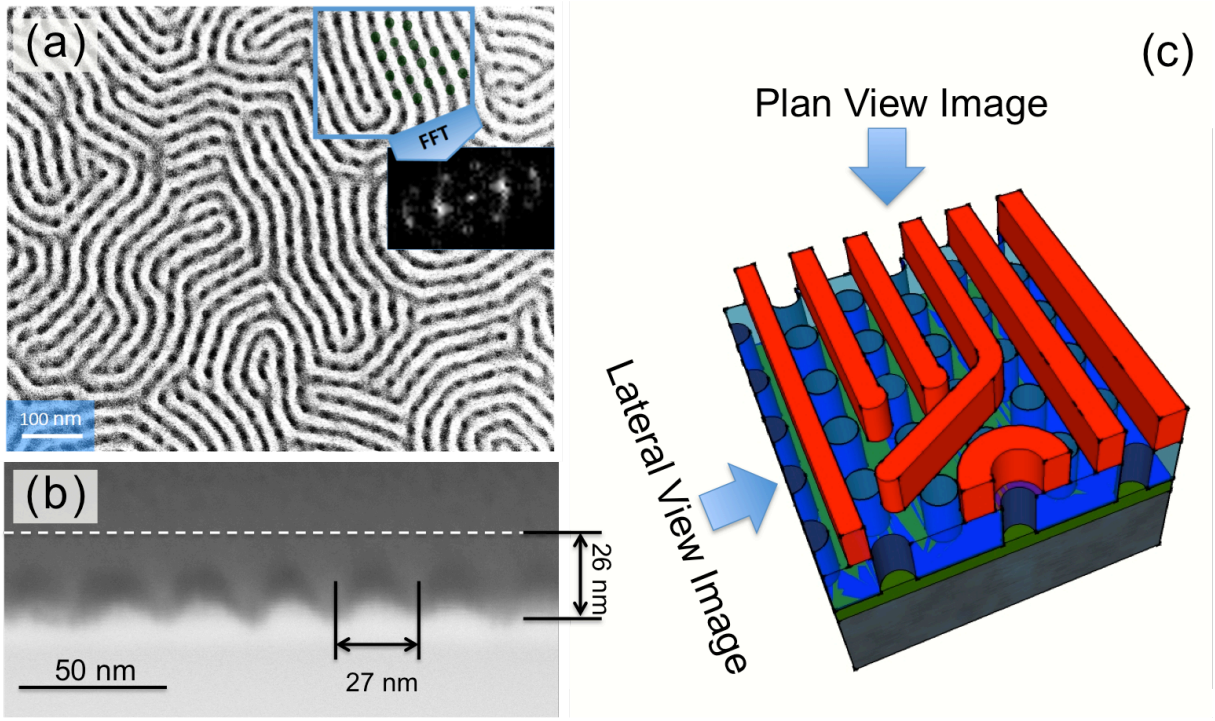

Fig. 4 SEM plan view (c) and STEM cross sectional (b) images of the sample annealed at 250°C for 60 s after prolonged oxygen plasma exposure. A cylindrical phase, perfectly registered with the lamellar pattern on the surface, is observed, as schematically sketched in the picture on the right (c).

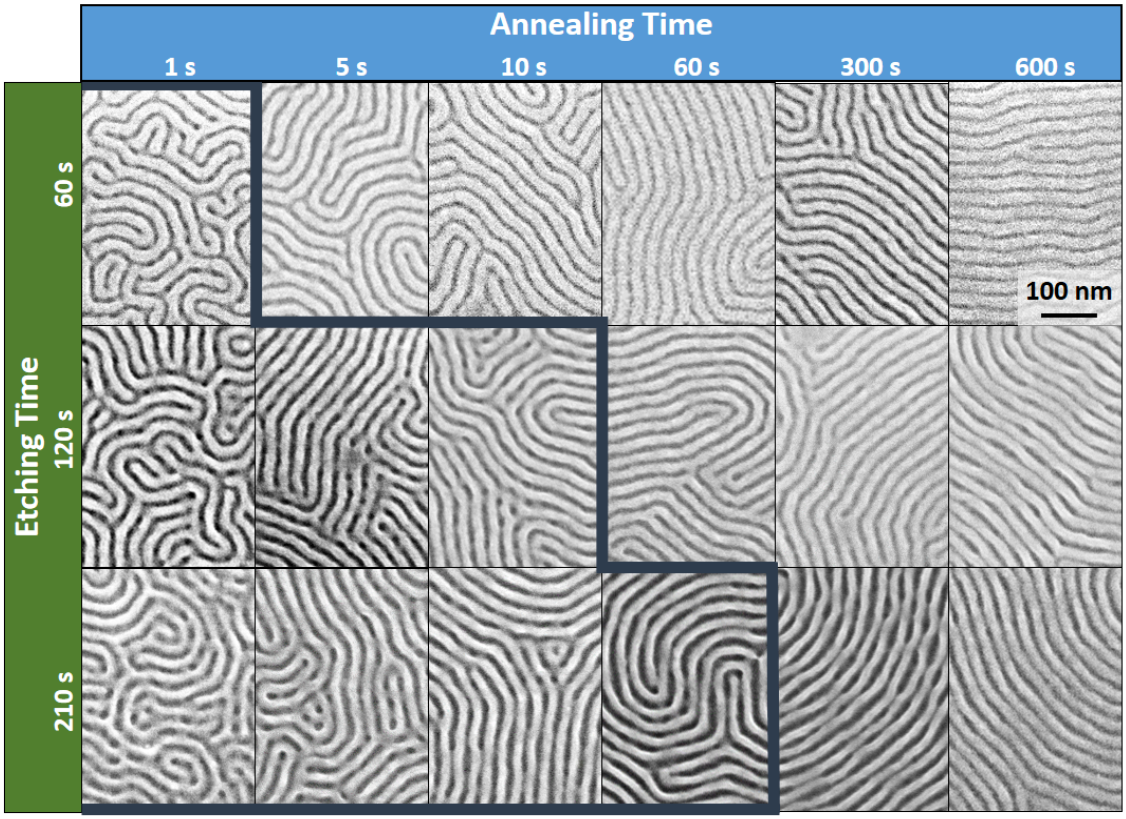

Fig. 5 Top-down SEM images of 30 nm thick B50 films annealed at 290°C for times ranging from 1 to 600 s after different oxygen plasma-etching times (60, 120, and 210 s). The blue line highlights the samples in which the presence of a cylindrical phase registered with the lamellar structure is observed.

peculiar behavior was already noticed in confined BCP thin films treated via solvent annealing[38], but was never reported to occur during conventional thermal treatments. The mechanism underlying this evolution of the nanodomain orientation was identified and directly connected to the progressive de-swelling of the film, due to progressive desorption, during the thermal treatment, of the solvent naturally retained in the film. On the basis of these experimental evidences, all the steps involved in the sample preparation were reconsidered from the residual toluene point of view. The absolute amount of toluene in the polymer films was determined by GC-MS analysis after proper extraction in dichloromethane. The extraction conditions were found extremely critical and very long extraction times should be employed. For clarity, all the results are expressed in terms of relative volume amount (V_r) of toluene using the toluene bulk density whereas all the data, including the absolute amount of toluene and the geometric characteristics of the films are reported in the Supporting Information.

The relative volume amount of toluene after spinning R58, but before the thermal treatment to perform the grafting reaction, is V_r = 5.9 ± 0.4 % which reduces to V_r = 4.5 ± 0.1 % after the RTP treatment at 250°C for 600 s. It is interesting to note that although the grafting treatment in RTP is performed at high temperature, the decrease of toluene content is quite limited thus indicating that the toluene is strongly retained in the random copolymer layer. After the washing step to remove the non-grafted R58 fraction, the toluene amount increases up to V_r = 23.5 ± 0.3 %. The block copolymer B50 was then spin coated on the above random layer and the total amount of toluene averaged over the total thickness of the film, which includes both the random and the block copolymer layers, results V_r = 26.2 ± 0.3 %. This data clearly indicates that the amount of naturally trapped solvent within an ultrathin polymer layer is very high prior to thermal treatments.

Numerous studies were performed to address the solvent retention and distribution in polymeric films. In as-cast thin polystyrene films[39], the mass fraction of residual toluene was determined by GC, and increased from 2% to 35% with decreasing film thickness (500 to 15 nm). In addition, the amount of toluene reduced to 9% percent after annealing at 115°C for 16 h, thus indicating that the solvent is retained even in dried films. This finding was also confirmed[40] in absorption/desorption experiments of toluene in several methacrylate polymer films, where some toluene remains trapped even after heating to 50°C for 12 h. Neutron reflectivity, employed to determine the amount of residual solvent in PS,[41,42] PMMA[42] as well as in PS-b-PMMA samples,[43,44] confirmed that a significant amount of toluene as residual solvent (9% to 15% volume fraction) remains in as-cast films after spin coating. The solvent evaporation during the spin coating process results in an increase in the polymer concentration at the polymer-air surface thus ultimately leading to the formation of a vitrified skin. In turn, the presence of this skin creates a barrier for further solvent evaporation thus inhibiting transport of solvent out from the film. Consequently, the concentration of the solvent at the polymer-air surface is the lowest one and a gradient in the solvent concentration should develop normal to the surface. In addition, a tendency for the solvent to accumulate near the solid substrate was suggested,[39] due to entropy effects.

To understand the solvent dynamics in the present system, three series of samples, consisting of the block copolymer spin coated on the grafted random copolymer layer, were prepared with exactly the same procedure and were subjected to RTP processing at the same temperatures and for the same time periods of the samples for which the correlation lengths were estimated. Figure 6 reports the relative volume amount V_r of toluene at 250, 270, and 290°C as a function of t_a. During the thermal treatment consisting in heating the sample at 18°C/s from room temperature to T_a followed by 1 s at T_a and cooling to room temperature, a significant reduction of the solvent content is observed, thus indicating the occurrence of a fast evaporation of the solvent. When T_a is 250°C, the solvent amount reduces by 40% of the initial value whereas more than 70% of the solvent evaporates when T_a is 290°C. A slight but continuous decrease of the residual toluene is further observed at all temperatures when increasing the annealing time. At the end of the RTP process, a significant amount of residual toluene is still present, ranging from 10 to 7% corresponding to the annealing temperature of 250 and 290°C, respectively. These data indicates that the solvent evaporation occurs in two distinct stages. A fast stage during heating to the annealing temperature followed by a relatively slow stage once this temperature is reached.

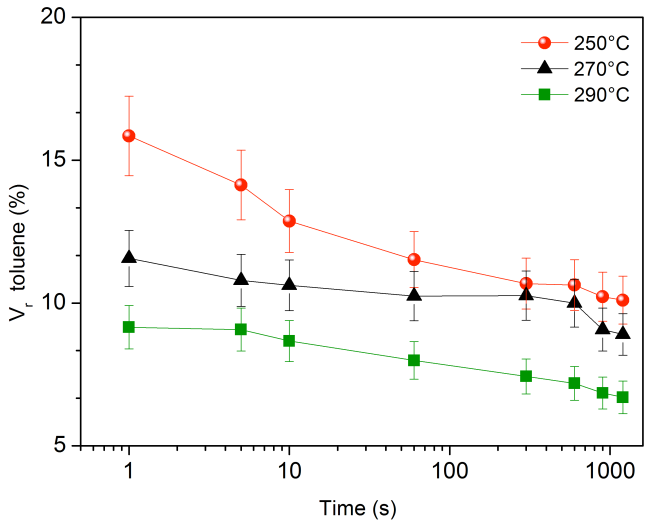

Fig. 6 Relative volume amount of toluene in B50 thin films deposited on R58 brush layers as a function of annealing time at different temperatures.

Ordering mechanism. Comparison of the solvent dynamics with the pattern and morphology evolution clearly indicates that the residual toluene strongly biases the ordering mechanism. Figure 7 depicts a schematic diagram that correlates the morphology evolution of the polymeric film with the progressive desorption of the solvent within the layer during the RTP treatment. The experimental data bears out a significant reduction of solvent content during the initial heating period of the thermal treatment. In agreement with a previously proposed ordering mechanism driven by solvent evaporation,[45] the burst of solvent is expected to cause an ordering front to propagate throughout the film and to provide a field gradient which assists the perpendicular orientation of the phase separated structures. At the same time, a solvent gradient develops across the layer. The lowest toluene concentration is expected to be located at the free surface of the film while the maximum concentration is located at the polymer/substrate interface. In this context, it is relevant to notice that the toluene amount in the layers of the random and block copolymers could be different, implying a more complex solvent concentration profile along the film. Anyway, such a solvent gradient accounts for the occurrence of the closely connected lamellar and cylinder structures. Indeed in the solvent-poor region of the film close to the free surface, the phase separation results in the formation of lamellar structures as expected for symmetric block copolymers. Conversely, inside the solvent-rich polymer/substrate interface, as toluene is a preferential solvent for PS, a selective partitioning occurs with preferential swelling for the PS block. This causes an increase in the relative volume fraction of the PS blocks and, when the toluene concentration is sufficiently high, the differential volume change in the swollen state of the PS and PMMA blocks leads to a local order-to-order transition from the expected lamellar morphology to the cylinder one, thus ultimately producing a self-registered structure with lamellae at the upper side of the film and cylinders at the lower side. The progressive solvent evaporation, which occurs during the isothermal annealing period, decreases the differential volume change between the swollen PS and PMMA blocks making the cylinder phase metastable so that the PMMA cylinders evolve into lamellae thus progressively moving vertically down the lamellae/cylinder interface until the random layer is reached and the cylinder structure totally disappears. A clear correlation between the solvent content and the evolution of this double morphology can be obtained looking at the

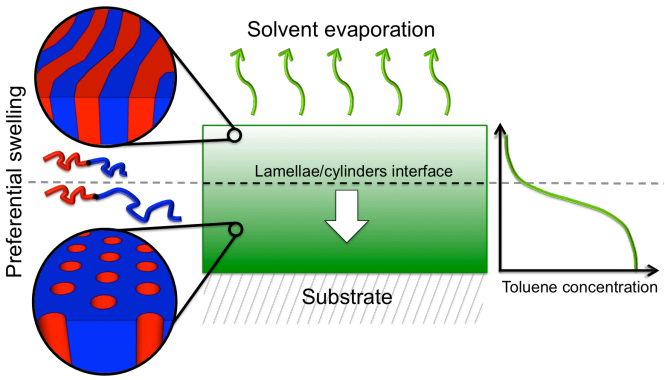

Fig. 7 Schematic diagram of the solvent evaporation and morphological evolution in the block copolymer thin film during RTP treatment. A gradient in the concentration of the solvent is established normal to the film surface with the solvent concentration progressively increasing with depth. This increase in solvent concentration induces a preferential swelling of the PS component in the macromolecules close to the film/substrate interface thus leading to a transition from lamellar to cylindrical phase through the film thickness. As the solvent evaporates, the order-to-order transition front propagates through the film producing highly ordered and perpendicularly oriented lamellar microdomains.

images of the sample annealed for 1 s at different temperatures that are reported in figure 3. Apart from the different level of lateral ordering achieved in the superficial lamellar structure, the investigation of the in depth morphology, performed by increasing the duration of the O_2 plasma treatment, revealed a variation of the relative volume occupied by the two phases in the polymeric film: higher the annealing temperature, lower the solvent content, deeper the propagation of the superficial lamellar phase in the polymeric film.

This vanishing cylindrical phase plays a fundamental role in the ordering kinetic of the lamellae. As previously discussed, pattern coarsening in symmetric block copolymer thin film is usually limited by topological constrains resulting in a quite slow kinetics. For perpendicular lamellae, the correlation length values ξ are reported not to change significantly with time and temperature. In particular, growth exponents $\phi \sim 0.02$ and $\phi \sim 0.14$ are reported for PS-b-PMMA block copolymers with molecular weight M_n = 46 kg/mol and M_n = 32 kg/mol, respectively.[8] Conversely, cylinder forming asymmetric block copolymers exhibit a faster ordering kinetic since their topological structure provides an alternative path for layer breaking thus significantly decreasing the energy barrier for defect annihilation and consequently boost the coarsening process in this system.[8] Coarsening in cylinder forming block copolymers has been investigated by several authors both in bulk phase and in thin films. Bulk cylindrical phase block copolymers have been reported[46] to coarsen with a power law $\xi \propto t^{1.06}$. Harrison et al. first reported a growth exponent $\phi \sim 0.25$ for asymmetric block copolymer thin films with parallel orientation of the cylinders with respect to the substrate.[23] Based on topological considerations, the coarsening kinetic exponent in asymmetric block copolymer thin film has been predicted to be limited to 1/4 in the infinite time limit under isotropic annealing condition. It is worth to note that the ϕ values we measured in the fast coarsening regime are systematically larger than the one expected according to the theoretical predictions. Nevertheless several authors reported similar growth exponent $\phi \sim 0.28$ in asymmetric block copolymer with cylinder perpendicularly oriented with respect to the substrate, suggesting the possibility that slightly different defect dynamics could apply when changing sample geometries.[25,27]

In the present system, two distinct growth regimes are clearly identified. Initially, the correlation length evolves rapidly following a power law $\xi \propto t^{0.29}$. Then, a slope change in the log ξ vs log time and coarsening slows down with a growth exponent $\phi \sim 0.03$. This double regime is strictly related to the evolution of the cylinders at the base of the lamellar phase. The initial fast coarsening regime of the lamellar phase is driven by the underlying cylindrical phase with a growth exponent $\phi \sim 0.29$, which is equivalent to those reported in previous experiments for perpendicular-oriented cylindrical phase block copolymers.[25,27] Then, the cylinder phase disappears and the evolution of the lamellae is limited by the previously described topological constrains and the growth exponent equals those reported in literature for symmetric block copolymer thin films.[8,23]

In this context, it is important to notice that fast coarsening in lamellar block copolymer thin films has already been demonstrated by different authors introducing a pre-patterning of the substrate that drives the self-assembly process of the macromolecules deposited on top of it.[12–14,19] Interestingly, a double layer approach has been effectively used in order to achieve high correlation length lamellar pattern.[9] The parallel oriented cylindrical phase PS-b-PMMA was formed and subsequently immobilized by PS crosslinking via UV irradiation. This layer was successfully used as a template to guide the top layer of perpendicularly oriented lamellar phase of PS-b-PMMA block copolymers. The final correlation length of the lamellar film coarsens with annealing time and asymptotically approaches that of the respective under layer film with final values much higher than the ones observed in single layer of lamellar film. These results indicate that in specific conditions, by properly modulating the surface energy of the substrate, high correlation length values and fast coarsening in symmetric block copolymer thin films are possible. However, the picture delineated in the present work is substantially different since the coarsening dynamics of the lamellae is essentially driven by the internal evolution of the system that experience an order-to-order transition determined, at the end, by the progressive desorption of residual solvent originally trapped in the film during the deposition process. In this picture, the cylindrical phase does not simply act as a template that guide the ordering process in the lamellar phase, but actively participates in the evolution of the system, providing alternative paths for macromolecules diffusion and resulting in a significant reduction of the enthalpy barrier for defect annihilation.

Conclusions

The pattern coarsening dynamics in symmetric PS-b-PMMA block copolymer thin films, subjected to rapid thermal processing (RTP), is delineated from 250 to 290°C. Within this temperature range, the correlation length increases steeply at first and then more gradually, with a well defined threshold, which depends on the temperature, thus indicating the occurrence of two distinct growth regimes. These two regimes are characterized by power laws with markedly different growth exponents (ϕ). In the fast coarsening regime, the evolution of the correlation length follows a power law with the growth exponent $\phi = 0.32$ typical for sphere or cylinder forming asymmetric block copolymers but never reported for symmetric block copolymers. In contrast, in the slow coarsening regime ϕ values below 0.10 are measured, in perfect agreement with the growth exponent reported in the literature for lamellae forming symmetric block copolymers. These results correlated with the presence, within the polymeric film, of a peculiar morphology involving periodic lamellae laying registered over a hexagonal pattern of PMMA cylinders embedded in the PS matrix and perpendicularly oriented with respect to the substrate. The origin of the two connected phases is related to the presence of a consistent amount of toluene, which is naturally entrapped in the film after the spinning process. Due to the preferential selectivity of toluene for the PS block, a differential swelling occurs leading to the formation of cylinders of PMMA embedded into a PS matrix in the toluene reach regions. The evolution of these two structures is governed by desorption of the solvent in the film during the thermal treatment. As the solvent evaporates the cylinder phase becomes unstable, and an order-to-order transition front propagates through the film thus ultimately producing highly ordered and perpendicularly oriented lamellar microdomains.

These data configure the RTP treatment as a solvent assisted thermal annealing process and demonstrate that very fast coarsening of lamellar PS-b-PMMA block copolymers can be achieved in RTP treated samples, elucidating the intimate

mechanism of lateral ordering in lamellar phase block copolymer. From a technological point of view, understanding the self-assembly process in block copolymer thin films provides insight into practical approaches for improving long-range order and reducing defect density, as required in the directed self-assembly of block copolymers using chemically or topographically patterned surfaces. In this regard, the present work represents a further step toward the exploitation of lamellae forming block copolymers for lithographic applications involving striped patterns.

Acknowledgement

This research activity was partially funded by the ERANET PLUS "NanoSci-E+" consortium through the NANO-BLOCK project, and by the European Metrology Research Programme (EMRP), project new01-TReND. The EMRP is jointly funded by the EMRP participating countries within EURAMET and the European Union. Patent protection related to this work is pending.

Notes and references

[a] Laboratorio MDM, IMM-CNR, Via C. Olivetti 2, Agrate Brianza 20864, Italy

[b] Dipartimento di Fisica, Università degli Studi di Milano, Via Celoria 16, Milano 20133, Italy

[c] Nano Facility Piemonte, Electromagnetism Division, Istituto Nazionale di Ricerca Metrologica Strada delle Cacce 91, Torino 10135, Italy

[d] Dipartimento di Scienze e Innovazione Tecnologica (DISIT), Viale T. Michel 11, Università del Piemonte Orientale ''A. Avogadro'', INSTM, UdR Alessandria, Alessandria 15121, Italy

1. S. B. Darling, Prog. Polym. Sci., 2007, **32**, 1152–1204.
2. K. Koo, H. Ahn, S.-W. Kim, D. Y. Ryu, and T. P. Russell, *Soft Matter*, 2013, **9**, 9059–9071.
3. Q. Peng, Y.-C. Tseng, S.B. Darling, J.W. Elam, *Adv Mater.*, 2010, **22** 5129.
4. Q. Peng, Y.-C. Tseng, S.B. Darling, J.W. Elam, *ACS Nano*, 2011, **5** 4600-4606.
5. Y.-C. Tseng, Q. Peng, L.E. Ocola, J.W. Elam, S. B. Darling, *J. Phys. Chem. C*, 115 (2011) 17725-17729.
6. C. Castro, S. Schamm-Chardon, B. Pecassou, A. Andreozzi, G. Seguini, M. Perego, G. BenAssayag, *Nanotechnology*, 2011, **24**, 075302.
7. A. Andreozzi, G. Seguini, M. Fanciulli, L. Lamagna, Celia Castro, Sylvie Schamm-Chardon, M. Perego, *Nanotechnology*, 2011, 22, 335303.
8. R. Ruiz, J. Bosworth, and C. Black, Phys. Rev. B, 2008, **77**, 054204.
9. R. Ruiz, R. L. Sandstrom, and C. T. Black, *Adv. Mater.*, 2007, **19**, 587–591.
10. S.-M. Park, M. P. Stoykovich, R. Ruiz, Y. Zhang, C. T. Black, and P. F. Nealey, *Adv. Mater.*, 2007, **19**, 607–611.
11. R. Ruiz, N. Ruiz, Y. Zhang, R. L. Sandstrom, and C. T. Black, *Adv. Mater.*, 2007, **19**, 2157–2162.
12. L. Rockford, Y. Liu, P. Mansky, T. Russell, M. Yoon, and S. Mochrie, *Phys. Rev. Lett.*, 1999, **82**, 2602–2605.
13. S. O. Kim, H. H. Solak, M. P. Stoykovich, N. J. Ferrier, J. J. De Pablo, and P. F. Nealey, *Nature*, 2003, **424**, 411–414.
14. M. P. Stoykovich, M. Müller, S. O. Kim, H. H. Solak, E. W. Edwards, J. J. de Pablo, and P. F. Nealey, *Science*, 2005, **308**, 1442–1446.
15. I. P. Campbell, S. Hirokawa, and M. P. Stoykovich, *Macromolecules*, 2013, **46**, 9599–9608.
16. S. O. Kim, B. H. Kim, K. Kim, C. M. Koo, M. P. Stoykovich, P. F. Nealey, and H. H. Solak, *Macromolecules*, 2006, **39**, 5466–5470.
17. K. W. Gotrik and C. A. Ross, *Nano Lett.*, 2013, 13, 5117–22.
18. V. Mishra, G. H. Fredrickson, and E. J. Kramer, *ACS Nano*, 2012, **6**, 2629–2641.
19. A. M. Welander, H. Kang, K. O. Stuen, H. H. Solak, M. Müller, J. J. De Pablo, and P. F. Nealey, *Macromolecules*, 2008, **41**, 2759–2761.
20. C.K. Jeong, H.M. Jin, J.-H. Ahn, T.J. Park, H.G. Yoo, M. Koo, Y.-K. Choi, S.O. Kim, K.J. Lee, *Small,* 2014, **10**(2), 337–343.
21. C. Garozzo, C. Bongiorno, S. Di Franco, M. Italia, A. La Magna, S. Scalese, P.M. Sberna, R.A. Puglisi, *Physica status solidi (a),* 2013, **210**(8), 1564–1570.
22. J. Tang, H.-T. Wang, D.H. Lee, M. Fardy, Z. Huo, T.P. Russell, P. Yang, *Nano Lett.*, 2010, **10**(10), 4279–4283.
23. C. Harrison, D. H. Adamson, Z. Cheng, J. M. Sebastian, S. Sethuraman, D. A. Huse, R. A. Register, and P. M. Chaikin, *Science*, 2000, **290**, 1558.
24. C. Harrison, Z. Cheng, S. Sethuraman, D. Huse, P. Chaikin, D. Vega, J. Sebastian, R. Register, and D. Adamson, *Phys. Rev. E*, 2002, **66**, 011706.
25. S. Ji, C. Liu, W. Liao, A. L. Fenske, G. S. W. Craig, and P. F. Nealey, *Macromolecules*, 2011, **44**, 4291–4300.
26. X. Zhang, K. D. Harris, N. L. Y. Wu, J. N. Murphy, and J. M. Buriak, *ACS Nano*, 2010, **4**, 7021–7029.
27. C. T. Black and K. W. Guarini, J. Polym. Sci., 2003, 42, 1970–1975.
28. B. C. Berry, A. W. Bosse, J. F. Douglas, R. L. Jones, and A. Karim, *Nano Lett.*, 2007, **7**, 2789–94.
29. F. Ferrarese Lupi, T. J. Giammaria, M. Ceresoli, G. Seguini, K. Sparnacci, D. Antonioli, V. Gianotti, M. Laus, and M. Perego, *Nanotechnology*, 2013, **24**, 315601.
30. F. Ferrarese Lupi, T. J. Giammaria, G. Seguini, M. Ceresoli, M. Perego, D. Antonioli, V. Gianotti, K. Sparnacci, and M. Laus, *J. Mater. Chem. C*, 2014, DOI:10.1039/C4TC00328D.
31. V. Gianotti, D. Antonioli, K. Sparnacci, M. Laus, T. J. Giammaria, F. Ferrarese Lupi, G. Seguini, and M. Perego, *Macromolecules*, 2013, **46**, 8224–8234.
32. C. Harrison, P. M. Chaikin, D. A. Huse, R. A. Register, D. H. Adamson, A. Daniel, E. Huang, P. Mansky, T. P. Russell, C. J. Hawker, D. A. Egolf, I. V. Melnikov, and E. Bodenschatz, *Macromolecules*, 2000, **33**, 857–865.
33. Y.-H. Ting, S.-M. Park, C.-C. Liu, X. Liu, F. J. Himpsel, P. F. Nealey, and A. E. Wendt, *J. Vac. Sci. Technol. B Microelectron. Nanom. Struct.,* 2008, **26**, 1684–1689.
34. S. Sakurai, T. Momii, K. Taie, M. Shibayama, S. Nomura, and T. Hashimoto, *Macromolecules*, 1993, **26**, 485–491.
35. C. M. Hansen, Hansen Solubility Parameters, *A User's Handbook;, CRC Press: Boca Raton*, FL, 2000.
36. J. Gong, H. Ahn, E. Kim, H. Lee, S. Park, M. Lee, S. Lee, T. Kim, E. A. Kwak, and D. Y. Ryu, *Soft Matter*, 2012, **8**, 3570–3575.
37. F. Ferrarese Lupi, T. J. Giammaria, G. Seguini, M. Laus, E. Enrico, N. De Leo, L. Boarino, C. K. Ober, and M. Perego, *J. Mater. Chem. C*, 2014, **2**, 2175.
38. P. Mokarian-Tabari, T. W. Collins, J. D. Holmes, and M. a Morris, *ACS Nano*, 2011, **5**, 4617–4623.
39. J. García-Turiel and B. Jérôme, *Colloid Polym. Sci.*, 2007, 285, 1617–1623.
40. A. Saby-Dubreuil, B. Guerrier, C. Allain, and D. Johannsmann, *Polymer*, 2001, **42**, 1383–1391.
41. J. Perlich, V. Korstgens, E. Metwalli, L. Schulz, R. Georgii, and P. Muller-Buschbaum, *Macromolecules*, 2009, **42**, 337–344.
42. X. Zhang, K. G. Yager, S. Kang, N. J. Fredin, B. Akgun, S. Satija, J. F. Douglas, A. Karim, and R. L. Jones, *Macromolecules*, 2010, **43**, 1117–1123.
43. X. Zhang, B. C. Berry, K. G. Yager, S. Kim, R. L. Jones, S. Satija, D. L. Pickel, J. F. Douglas, and A. Karim, *ACS Nano*, 2008, **2**, 2331–2341.
44. X. Zhang, J. F. Douglas, and R. L. Jones, *Soft Matter*, 2012, **8**, 4980–4987.
45. S. H. Kim, M. J. Misner, T. Xu, M. Kimura, and T. P. Russell, *Adv. Mater.*, 2004, **16**, 226–231.
46. H. Dai, N. Balsara, B. Garetz, and M. Newstein, *Phys. Rev. Lett.*, 1996, **77**, 3677–3680.